Anharmonic coupling of the CH-stretch and CH-bend vibrations of chloroform as studied by near-infrared electroabsorption spectroscopy

Jun Nishida, Shinsuke Shigeto, Sohshi Yabumoto, and Hiro-o Hamaguchi

Citation: The Journal of Chemical Physics **137**, 234501 (2012); doi: 10.1063/1.4770264
View online: http://dx.doi.org/10.1063/1.4770264
View Table of Contents: http://scitation.aip.org/content/aip/journal/jcp/137/23?ver=pdfcov
Published by the AIP Publishing

Anharmonic coupling of the CH-stretch and CH-bend vibrations of chloroform as studied by near-infrared electroabsorption spectroscopy

Jun Nishida,[1,a)] Shinsuke Shigeto,[2,b)] Sohshi Yabumoto,[2,c)] and Hiro-o Hamaguchi[1,2]
[1]*Department of Chemistry, School of Science, The University of Tokyo, 7-3-1 Hongo, Bunkyo-ku, Tokyo 113-0033, Japan*
[2]*Department of Applied Chemistry and Institute of Molecular Science, National Chiao Tung University, 1001 Ta-Hsueh Road, Hsinchu 30010, Taiwan*

(Received 1 October 2012; accepted 26 November 2012; published online 19 December 2012)

Combination bands that involve CH- or OH-stretch vibrations appear in the near-infrared (NIR) region (4000–10 000 cm^{-1}). Because they arise from anharmonic coupling between the component fundamentals, detailed analysis of the frequency and intensity of NIR combination bands allows one to elucidate the mechanisms behind the vibrational coupling in the condensed phase in terms of mechanical and electrical anharmonicities. Nevertheless, little has been studied, in particular experimentally, on the origin of the combination band intensity. Here, we show that NIR electroabsorption (EA) spectroscopy, which directly probes the effects of an externally applied electric field on a combination band, can shed new light on anharmonic vibrational coupling through determination of the direction of the transition moment for the combination band. We studied the combination band of the CH-stretch (ν_1) and CH-bend (ν_4) modes of liquid chloroform. The electric-field induced absorbance change of the $\nu_1 + \nu_4$ combination band caused by reorientation of the chloroform molecule was measured at various χ angles, where χ is the angle between the direction of the applied electric field and the polarization of the incident IR light. We were able to detect an absorbance change as small as 5×10^{-8} for the combination band. Using the NIR EA spectra of the combination band together with those of the CH-stretch and bend fundamentals, the angle between the transition moment for the combination band and the permanent dipole moment was determined experimentally for the first time to be $(79 \pm 14)^\circ$. The present investigation indicates that the contribution of the CH-stretch mode to the mechanical anharmonicity is minor and that the CH-bend mode plays a dominant role in the mechanical part of the vibrational coupling between the two fundamentals. Furthermore, density functional theory calculations show that both the mechanical anharmonicity of the CH-bend mode and the electrical anharmonicity may contribute equally to the anharmonic coupling. © *2012 American Institute of Physics*. [http://dx.doi.org/10.1063/1.4770264]

I. INTRODUCTION

Anharmonic coupling between different vibrational modes plays a vitally important role in intra- and intermolecular interactions and molecular dynamics in the condensed phase. It has been shown to substantially influence the pathways and rates of vibrational energy relaxation in liquids and solutions.[1–4] Vibrational energy often relaxes preferentially through anharmonically coupled vibrations. In complex macromolecular systems such as polypeptides and proteins, the coupling of modes that are localized at specific locations is one of the key factors that dictate higher-order (secondary, tertiary, and so forth) structures in their equilibrium state.[5,6] Therefore, understanding the detailed mechanisms of anharmonic coupling not only lends deeper insight into the anharmonic nature of molecular vibrations, but it may also enable one to link the vibrational properties of molecules with the global molecular structure and its time evolution, just as in NMR methods.[7]

Anharmonic coupling can manifest itself in many ways. In coherent two-dimensional (2D) infrared (IR) spectroscopy, which has been developed and extensively used in the last decade, it is evidenced by the occurrence of cross-peaks in 2D spectra.[6,8–12] However, the simplest manifestation of anharmonic coupling between two modes is arguably combination bands observed with conventional linear vibrational spectroscopy. A combination band occurs when vibrational quanta of two or more modes are excited simultaneously. Whereas most of the fundamental transitions are observed in the mid-IR (MIR) region (800–4000 cm^{-1}), combination bands involving CH- or OH-stretch vibrations appear in the near-IR (NIR) region (4000–10 000 cm^{-1}).[13] A combination transition observed in a NIR spectrum, like any optical transitions, is characterized by its peak frequency and intensity. The combination frequency is usually redshifted with respect to the sum of the frequencies of the component fundamentals. The frequency shifts have been used as a convenient indicator of the degree of anharmonicity. On the other hand, the intensities of combination bands remain largely unexplored with NIR spectroscopy; NIR spectra alone do not allow one to

[a)]Present address: Department of Chemistry, Stanford University, California 94305, USA.
[b)]Author to whom correspondence should be addressed. Electronic mail: shigeto@mail.nctu.edu.tw.
[c)]Present address: Tokyo Instruments, Inc. Tokyo, Japan.

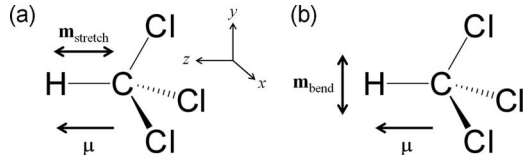

FIG. 1. CH-stretching (a) and CH-bending (b) modes of chloroform. The molecule-fixed coordinate system is also shown, in which the z-axis is taken along the CH bond. The permanent dipole moment of the molecule, $\boldsymbol{\mu}$, and the transition moment for the CH-stretching mode, $\mathbf{m}_{\text{stretch}}$, are parallel to the z-axis, whereas the transition moment for the CH-bending mode, $\mathbf{m}_{\text{bend}}$, is perpendicular to the z-axis.

access information on the physical origin of the intensity of a given combination band and hence on the underlying coupling mechanisms.

Here, we present NIR electroabsorption (EA) spectroscopy as a novel experimental approach to study anharmonic vibrational coupling in liquids and solutions through determination of the direction of the transition moment with respect to the permanent dipole moment of the molecule. By integrating a high-throughput NIR spectrometer used in our nanosecond time-resolved IR experiments[14–16] into an existing MIR EA apparatus,[17,18] we extend EA spectroscopy to cover the NIR region so that the electric-field effects on combination bands and overtones can be studied. In the present study, we focus on the combination band of the CH-stretching (ν_1) mode at 3019 cm^{-1} and doubly degenerate CH-bending (ν_4) mode at 1215 cm^{-1} of liquid chloroform (see Fig. 1). Chloroform has been studied as a model system for understanding anharmonic coupling in molecular liquids. The nine normal modes of chloroform, which form a basis for the spectral analysis of combination bands, are all well characterized.[19] It does not have the complications associated with hydrogen bonds. In addition to steady-state spectroscopy, high-quality ultrafast data of vibrational relaxation in liquid chloroform, both experimental[20,21] and theoretical,[22] are available in the literature. Chloroform (and its deuterated isotopomer) has also been studied with nonlinear vibrational spectroscopies.[23–29] From a technical viewpoint, the $\nu_1 + \nu_4$ transition is a relatively intense combination band and well suited for demonstration purposes.

In the rest of this paper, we first show that two types of anharmonicities, i.e., the mechanical and electrical anharmonicities, give rise to the transition moment of a combination band. We then describe molecular responses to an externally applied electric field that we observe in EA spectroscopy at room temperature. Of primary interest in the present study is absorption intensity changes, rather than peak shift or band broadening, induced by an applied electric field because they are directly associated with the angle between the transition moment and the permanent dipole moment. We present field-induced absorption difference (ΔA) spectra of the $\nu_1 + \nu_4$ combination band as well as the ν_1 and ν_4 fundamentals of liquid chloroform. A comprehensive analysis of those ΔA spectra has enabled us to experimentally determine the direction of the transition moment of the combination band. The vibrational anharmonicity that gives rise to the $\nu_1 + \nu_4$ combination band is discussed based on the NIR EA results together with density functional theory (DFT) calculation results.

II. THEORETICAL BACKGROUND

A. Mechanical and electrical anharmonicities in a combination transition

The intensity of an optical transition is proportional to the square modulus of the corresponding transition moment $\mathbf{m}$, defined as

$$\mathbf{m} = \langle \text{e} | \boldsymbol{\mu} | \text{g} \rangle , \tag{1}$$

where $\boldsymbol{\mu}$ is the dipole moment of the molecule of interest. $|\text{g}\rangle$ and $|\text{e}\rangle$ are the vibrational eigen kets of the ground and excited states, respectively. The transition moment for a fundamental transition (either ν_1 or ν_4) is obtained under the harmonic approximation as follows:

$$\mathbf{m}_{\text{fund}} = \langle 1 | Q | 0 \rangle \left(\frac{\partial \boldsymbol{\mu}}{\partial Q} \right)_0 = \frac{1}{\sqrt{2}} \left(\frac{\partial \boldsymbol{\mu}}{\partial Q} \right)_0 , \tag{2}$$

where Q is the dimensionless vibrational coordinate[8] of the fundamental [i.e., $Q = (m\omega/\hbar)^{1/2} q$ with q being the normal coordinate], $\hbar$ is Planck's constant h divided by 2π, and ω is the angular frequency of the vibration. Equation (2) shows that the transition moment of a fundamental is proportional to the dipole derivative, $(\partial \boldsymbol{\mu}/\partial Q)_0$, evaluated at the equilibrium geometry.

For the $\nu_1 + \nu_4$ combination transition, Eq. (1) can be written as

$$\begin{aligned} \mathbf{m}_{\text{comb}} &= \langle 1, 1 | \boldsymbol{\mu} | 0, 0 \rangle \\ &\cong \left(\frac{\partial \boldsymbol{\mu}}{\partial Q_{\text{stretch}}} \right)_0 \langle 1, 1 | Q_{\text{stretch}} | 0, 0 \rangle \\ &\quad + \left(\frac{\partial \boldsymbol{\mu}}{\partial Q_{\text{bend}}} \right)_0 \langle 1, 1 | Q_{\text{bend}} | 0, 0 \rangle \\ &\quad + \left(\frac{\partial^2 \boldsymbol{\mu}}{\partial Q_{\text{stretch}} \partial Q_{\text{bend}}} \right)_0 \langle 1, 1 | Q_{\text{stretch}} Q_{\text{bend}} | 0, 0 \rangle , \end{aligned} \tag{3}$$

$$\equiv \mathbf{m}^{\text{MA}}_{\text{stretch}} + \mathbf{m}^{\text{MA}}_{\text{bend}} + \mathbf{m}^{\text{EA}}. \tag{4}$$

Here, the notation $|v_{\text{stretch}}, v_{\text{bend}}\rangle$ is used to represent the vibrational state in which vibrational quantum number of the CH-stretching mode Q_{stretch} is v_{stretch} and that of the CH-bending mode Q_{bend} is v_{bend}. In this notation, $|0, 0\rangle$ corresponds to the ground state and $|1, 1\rangle$ to the $\nu_1 + \nu_4$ combination state. As shown in Eq. (4), three terms contribute to the absorption intensity of the combination band. The first two terms $\mathbf{m}^{\text{MA}}_{\text{stretch}}$ and $\mathbf{m}^{\text{MA}}_{\text{bend}}$ would vanish if the wave functions $|0, 0\rangle$ and $|1, 1\rangle$ were those of the harmonic oscillator. For these terms to be nonzero, the potential function, V, of the molecule must be anharmonic and include the cubic and higher-order

terms as

$$\begin{aligned} V(Q_{\text{stretch}}, Q_{\text{bend}}) &= \frac{1}{2}\left(\frac{\partial^2 V}{\partial Q_{\text{stretch}}^2}\right)_0 Q_{\text{stretch}}^2 + \frac{1}{2}\left(\frac{\partial^2 V}{\partial Q_{\text{bend}}^2}\right)_0 Q_{\text{bend}}^2 \\ &+ \frac{1}{6}\Bigg[\left(\frac{\partial^3 V}{\partial Q_{\text{stretch}}^3}\right)_0 Q_{\text{stretch}}^3 \\ &+ 3\left(\frac{\partial^3 V}{\partial Q_{\text{stretch}}^2 \partial Q_{\text{bend}}}\right)_0 Q_{\text{stretch}}^2 Q_{\text{bend}} \\ &+ 3\left(\frac{\partial^3 V}{\partial Q_{\text{stretch}} \partial Q_{\text{bend}}^2}\right)_0 Q_{\text{stretch}} Q_{\text{bend}}^2 \\ &+ \left(\frac{\partial^3 V}{\partial Q_{\text{bend}}^3}\right)_0 Q_{\text{bend}}^3\Bigg] + \cdots. \end{aligned}$$

If the quartic and higher-order terms in this expansion are neglected, $\mathbf{m}_{\text{stretch}}^{\text{MA}}$ and $\mathbf{m}_{\text{bend}}^{\text{MA}}$ can be derived as follows:[30]

$$\mathbf{m}_{\text{stretch}}^{\text{MA}} = \frac{1}{4\hbar\omega_{\text{stretch}}}\left(\frac{\partial \boldsymbol{\mu}}{\partial Q_{\text{stretch}}}\right)_0 \left(\frac{\partial^3 V}{\partial Q_{\text{stretch}}^2 \partial Q_{\text{bend}}}\right)_0, \quad (5)$$

$$\mathbf{m}_{\text{bend}}^{\text{MA}} = \frac{1}{4\hbar\omega_{\text{bend}}}\left(\frac{\partial \boldsymbol{\mu}}{\partial Q_{\text{bend}}}\right)_0 \left(\frac{\partial^3 V}{\partial Q_{\text{stretch}} \partial Q_{\text{bend}}^2}\right)_0. \quad (6)$$

It follows from Eqs. (5) and (6) that nonvanishing $\mathbf{m}_{\text{stretch}}^{\text{MA}}$ and $\mathbf{m}_{\text{bend}}^{\text{MA}}$ require $(\partial^3 V/\partial Q_{\text{stretch}}^2 \partial Q_{\text{bend}})_0$ and $(\partial^3 V/\partial Q_{\text{stretch}} \partial Q_{\text{bend}}^2)_0$ to be nonzero. This type of anharmonicity is known as the mechanical anharmonicity.[31] In contrast, the third term in Eq. (4), $\mathbf{m}^{\text{EA}}$, does not vanish even under the harmonic oscillator approximation. But it requires a nonlinear dependence of the dipole moment on Q_{stretch} and Q_{bend} so that $(\partial^2 \mu/\partial Q_{\text{stretch}} \partial Q_{\text{bend}})_0 \neq 0$, which is commonly termed the electrical anharmonicity.[31] Using perturbation theory, we obtain $\mathbf{m}^{\text{EA}}$ as[30]

$$\mathbf{m}^{\text{EA}} = \frac{1}{2}\left(\frac{\partial^2 \mu}{\partial Q_{\text{stretch}} \partial Q_{\text{bend}}}\right)_0. \quad (7)$$

Both mechanical and electrical anharmonicities are not taken into account in conventional *ab initio* IR intensity calculations that are based on the double-harmonic approximation.

The intensity information on combination bands yielded by conventional linear NIR spectra is limited to $|\mathbf{m}_{\text{comb}}|^2$, thus making it very difficult to distinguish between the contributions of the three anharmonicity terms in Eq. (4). NIR EA spectroscopy can potentially alleviate this limitation by looking into the direction of a combination band. We note here that $\mathbf{m}_{\text{comb}}$ is the vector sum of the three components $\mathbf{m}_{\text{stretch}}^{\text{MA}}$, $\mathbf{m}_{\text{bend}}^{\text{MA}}$, and $\mathbf{m}^{\text{EA}}$. Its direction should have additional information that helps to identify, at least, which term(s) is dominant. As illustrated below, the angle η, between the transition moment and dipole moment can be experimentally determined by NIR EA spectroscopy.

As is clear from Eq. (3), the directions of the mechanical anharmonicity terms $\mathbf{m}_{\text{stretch}}^{\text{MA}}$ and $\mathbf{m}_{\text{bend}}^{\text{MA}}$ are the same as those of the transition moments of the fundamentals, $\mathbf{m}_{\text{stretch}}$ and $\mathbf{m}_{\text{bend}}$. They are dictated by the directions of the dipole derivatives, $(\partial \boldsymbol{\mu}/\partial Q_{\text{stretch}})_0$ and $(\partial \boldsymbol{\mu}/\partial Q_{\text{bend}})_0$. Therefore, $\mathbf{m}_{\text{stretch}}^{\text{MA}}$ is parallel to the permanent dipole moment, which is along the CH bond [$\eta = 0°$; Fig. 1(a)], whereas $\mathbf{m}_{\text{bend}}^{\text{MA}}$ is perpendicular to the permanent dipole moment [$\eta = 90°$; Fig. 1(b)]. The direction of $\mathbf{m}^{\text{EA}}$ is not that obvious. However, by simple symmetry consideration on the chloroform molecule discussed in Sec. IV E, η for $\mathbf{m}^{\text{EA}}$ is expected to be 90°.

B. Molecular responses observed in EA spectroscopy

In this subsection, we present two types of molecular responses to an external field[32] that may be observed in EA measurements: namely, orientational polarization (OP) and electronic polarization (EP).

1. Orientational polarization

The first response we consider is orientational polarization,[17,18,33,34] which is the primary concern in this paper. When liquid molecules having nonzero permanent dipole moment are subject to an external electric field, a small fraction of the molecules tend to align so that the dipole moment is parallel to the applied field. In room-temperature liquids, this alignment follows the Boltzmann distribution. This field-induced molecular alignment, in turn, leads to anisotropy in the interaction between the transition moment and the electric-field vector of polarized incident IR light. The resulting absorbance change ΔA, normalized by the original absorbance A, is given by[17]

$$\left(\frac{\Delta A}{A}\right)_{\text{OP}} = \frac{\gamma^2}{12}\left(1 - 3\cos^2\eta\right)\left(1 - 3\cos^2\chi\right) \quad (8)$$

with

$$\gamma = \frac{\mu F}{k_{\text{B}} T}. \quad (9)$$

Here, η is the angle between the transition moment $\mathbf{m}$ and the permanent dipole moment $\boldsymbol{\mu}$ ($\mu = |\boldsymbol{\mu}|$). χ is the angle between the direction of the applied field and the polarization of the incident IR light. In Eq. (9), F is the magnitude of the local electric field that is exerted on the molecules, k_{B} is the Boltzmann constant, and T is the temperature. Equation (8) indicates that the orientational polarization ΔA spectrum is identical in shape to the absorption spectrum without any peak shift and band broadening. If the signal originating from orientational polarization is extracted from an experimental ΔA spectrum at given χ, angle η can be calculated using Eq. (8) with known μ and F. Another important implication of Eq. (8) is that $(\Delta A/A)_{\text{OP}}$ varies according to $1 - 3\cos^2\chi$.

2. Electronic polarization

The electric-field effects on the electronic properties of molecules also give rise to IR absorbance changes. The ΔA spectrum arising from the electronic polarization is generally expressed as[35]

$$\begin{aligned} \Delta A(\tilde{\nu}) = F^2 \Bigg\{ & A_\chi A(\tilde{\nu}) + \frac{B_\chi}{15hc}\tilde{\nu}\frac{\mathrm{d}}{\mathrm{d}\tilde{\nu}}\left[\frac{A(\tilde{\nu})}{\tilde{\nu}}\right] \\ & + \frac{C_\chi}{30h^2c^2}\tilde{\nu}\frac{\mathrm{d}^2}{\mathrm{d}\tilde{\nu}^2}\left[\frac{A(\tilde{\nu})}{\tilde{\nu}}\right]\Bigg\}, \end{aligned} \quad (10)$$

where $\tilde{\nu}$ is the wavenumber and c is the speed of light. The $\Delta A(\tilde{\nu})$ consists of the frequency-weighted zeroth, first, and second derivatives of the absorption spectrum A. Detailed formulae for the coefficients A_χ, B_χ, and C_χ can be found in Refs. 35–38. In short, they are complicated functions of the Stark parameters such as the changes in dipole moment, $\Delta\boldsymbol{\mu}$, and polarizability, $\Delta\boldsymbol{\alpha}$, upon vibrational excitation ($v = 1 \leftarrow 0$), transition polarizability $\mathbf{A}$, and transition hyperpolarizability $\mathbf{B}$. $\mathbf{A}$ and $\mathbf{B}$ are defined as $\mathbf{m}(\mathbf{F}) = \mathbf{m} + \mathbf{A} \cdot \mathbf{F} + \mathbf{F} \cdot \mathbf{B} \cdot \mathbf{F}$. Here, we focus on the zeroth-derivative term in Eq. (10) because it competes with the orientational polarization signal [Eq. (8)] and needs to be separated. Assuming that the transition hyperpolarizability is negligible[39,40] (i.e., $\mathbf{B} = 0$) and that the reorientation of the molecules through $\boldsymbol{\alpha}$ and $\mathbf{A}$ is small compared with that through $\boldsymbol{\mu}$,[18] we have the electronic polarization contribution to the zeroth-derivative ΔA signal of the form

$$\left(\frac{\Delta A}{A}\right)_{\mathrm{EP}} = \frac{F^2}{30\,|\mathbf{m}|^2} \sum_{i,j} \left[10A_{ij}^2 - (1 - 3\cos^2\chi) \times (3A_{ii}A_{jj} + A_{ij}^2)\right], \tag{11}$$

where A_{ij} is the ij-element of the transition polarizability tensor $\mathbf{A}$ ($i, j = x, y, z$). $(\Delta A/A)_{\mathrm{EP}}$ has both χ-independent and χ-dependent terms with the latter exhibiting exactly the same $1 - 3\cos^2\chi$ dependence as the orientational polarization signal [see Eq. (8)]. The key to distinguishing between the orientational and electronic polarization contributions lies in the $\Delta A/A$ signal at $\chi = 54.7°$. If significant $\Delta A/A$ is observed at $\chi = 54.7°$, it implies that there is a substantial contribution from electronic polarization because only the electronic polarization can give rise to ΔA signals at this magic angle.

For our ultimate goal to derive the direction of transition moment, the contribution of electronic polarization has to be removed from the observed signal. A previous study showed that the absorbance change due to electronic polarization is negligible for the C=O stretch of liquid acetone, compared with that due to orientational polarization.[17] In this study, the $\nu_1 + \nu_4$ combination band of liquid chloroform is also found to be free from the contamination of electronic polarization (see Sec. IV B). In contrast, it turns out that in the case of the CH-stretching fundamental, both orientational and electronic polarizations contribute considerably to the field-induced absorbance change. Nevertheless, a reasonable approximation on the components of the tensor $\mathbf{A}$ further simplifies Eq. (11) and thereby makes it possible to evaluate the absorbance change that is attributed solely to the orientational polarization (see Sec. IV C 1).

III. METHODS

A. NIR EA spectroscopy

Combination bands are typically much weaker than fundamentals. The field-induced absorbance changes of combination bands are far weaker. To detect such exceedingly small changes in the NIR region, we combined a high-throughput near/mid-IR spectrometer and detection system used in our nanosecond time-resolved experiments[14–16] and the field application module that we have been using for the MIR EA apparatus described in detail previously.[17,18] The main feature of that apparatus is the use of a dispersive monochromator and alternating current (ac)-coupled amplification,[14–16] which affords detection of ΔA signals as small as 10^{-7}. In this work, the new spectrometer (JASCO CP-50TFP; focal length = 500 mm, f = 4.3) extended the spectral window for EA measurements to cover the 4000–12000 cm^{-1} region by using a 600 g/mm grating, while keeping the high sensitivity intact. The NIR light source was a tungsten lamp and the light emitted from the tungsten lamp was p-polarized using a wire-grid IR polarizer. The spectral resolution was 16 cm^{-1} to increase a signal-to-noise ratio (S/N). An InSb photodiode (Kolmar Technologies KISDP-1-J1/DC) was used as a detector for the combination band measurement. About 25 kHz (f), 80 $V_{0\text{-}p}$ AC voltage was applied across a sample cell and a 50 kHz ($2f$) AC component, which depends on the field strength quadratically, was selectively detected by a phase-sensitive lock-in amplifier (Stanford Research Systems SR844). The phase difference between the signal and reference in the lock-in amplifier was adjusted in every measurement so that out-of-phase ΔA signals were minimized. During measurement, liquid chloroform was flowed through a home-made sample cell, which was composed of a 6-μm-thick polyethylene terephthalate film spacer (Mitsubishi Plastics Diafoil®) sandwiched by two p-type boron doped silicon windows (Pier Optics; thickness = 0.5 mm, resistivity = 0.8–2 Ω cm). The two silicon windows also served as electrodes, but the surfaces in contact with the sample were coated by a thin layer of SiO_2 (thickness = 0.3 μm) for insulation. For measurements of the fundamental bands, the MIR EA spectrometer reported previously[17,18] was employed without modification; a photoconductive HgCdTe detector was used for the CH-bending mode, whereas the same InSb detector as above was used for the CH-stretching mode. The spectral resolution was 12 cm^{-1}. To achieve higher S/N, the IR absorption spectrum of liquid chloroform was also recorded with a JASCO FT/IR-6100 spectrometer.

HPLC-grade chloroform (≥99.8%) was commercially obtained from Sigma-Aldrich and used without further purification. Chloroform contains a trace amount of ethanol (typically 0.5%–1.0%) as a stabilizer, but no noticeable effect of ethanol was found in IR measurements. All measurements were performed at room temperature.

B. DFT calculation of the potential energy surface and dipole moment function

To help with understanding the anharmonic coupling mechanisms, DFT calculations were performed on an isolated chloroform molecule using the B3LYP functional[41,42] and the 6-31+G(d,p) basis set as implemented in GAUSSIAN 09.[43] A numerical integration grid of higher accuracy (Int = Ultrafine) was used. The potential energy surface $V(q_{\mathrm{stretch}}, q_{\mathrm{bend}})$ and dipole moment function $\mu(q_{\mathrm{stretch}}, q_{\mathrm{bend}})$ were calculated at nonequilibrium geometries by stepwise displacing the hydrogen atom from its equilibrium position along the q_{stretch} and q_{bend} coordinates at 0.01 Å intervals. The functions so obtained were fitted with two-dimensional

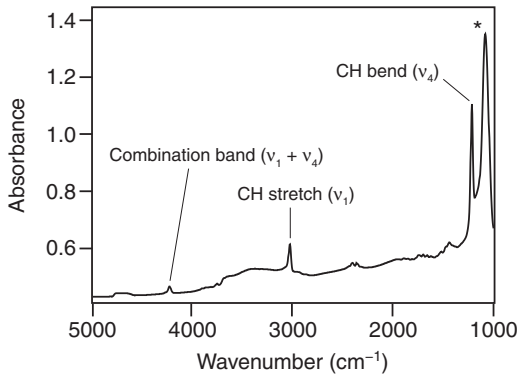

FIG. 2. FTIR spectrum of liquid chloroform. The CH-stretching (ν_1) mode is observed at 3019 cm^{-1}, the CH-bending (ν_4) mode at 1215 cm^{-1}, and their combination band ($\nu_1 + \nu_4$) at 4215 cm^{-1}. An offset in absorbance of 0.4–0.6 is due to the reflection of the incident IR light at the silicon windows. An asterisk denotes an intense band of SiO_2.

polynomials and the fitting coefficients were used to evaluate the derivatives $\partial^3 V/\partial q_{\text{stretch}}^2 \partial q_{\text{bend}}$, $\partial^3 V/\partial q_{\text{stretch}} \partial q_{\text{bend}}^2$, and $\partial^2 \mu/\partial q_{\text{stretch}} \partial q_{\text{bend}}$. Note that the calculations here were based on the normal coordinates q_{stretch} and q_{bend} instead of the reduced vibrational coordinates Q_{stretch} and Q_{bend}. Using the definition $Q = (m\omega/\hbar)^{1/2} q$, however, the derivatives with respect to q can be readily converted to those with respect to Q that are directly associated with the anharmonicity terms [Eqs. (5)–(7)].

IV. RESULTS AND DISCUSSION

A. Absorption spectrum of liquid chloroform

Figure 2 shows the IR spectrum of liquid chloroform. An offset of 0.4–0.6 is due to the reflection of the incident IR light at the silicon windows. Apart from an intense band of SiO_2 at around 1100 cm^{-1}, three prominent absorption bands of chloroform are seen in the spectrum. The bands at 3019 and 1215 cm^{-1} are assigned to the fundamentals of the CH-stretching (ν_1) and CH-bending (ν_4) modes, respectively. A very weak band observed at 4215 cm^{-1} is their combination band ($\nu_1 + \nu_4$). The anharmonic shift is found to be -19 cm^{-1}.

B. EA spectra in the combination band region

Figure 3 displays the NIR EA spectra of liquid chloroform in the $\nu_1 + \nu_4$ combination band region at six χ angles, together with the conventional FTIR spectrum measured with the home-made sample cell (as in Fig. 2). To our knowledge, this is the first report of EA of a combination band of molecular liquid. The EA spectra shown in this and subsequent figures have been baseline-corrected. The variation in optical path length with angle χ has been corrected by taking into account the refractive index of chloroform ($n = 1.44$). A positive ΔA signal of $\sim 1.0 \times 10^{-7}$ is clearly observed at $\chi = 90°$ and it decreases in going from $\chi = 90°$ to 58°. The ΔA signal at $\chi = 58°$ is as small as 5×10^{-8}, illustrating the high sensitivity of our apparatus also in the NIR region. Detection of such small ΔA signal would not be feasible at the present stage with the dc method using FTIR.

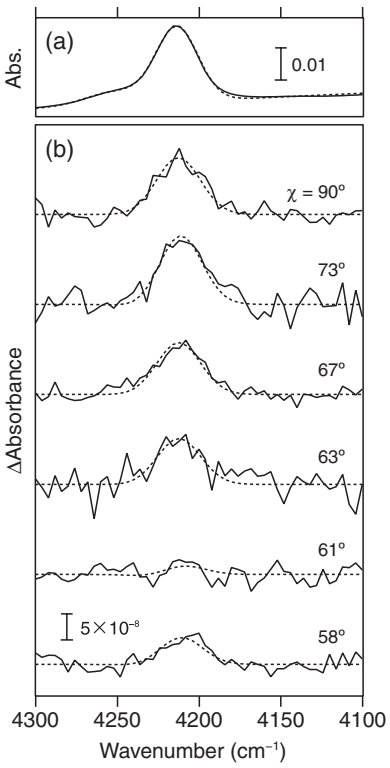

FIG. 3. IR spectrum (a) and EA spectra (b) of liquid chloroform in the $\nu_1 + \nu_4$ combination band region. The EA spectra were measured at $\chi = 58°$, 61°, 63°, 67°, 73°, and 90° (normal incidence). Solid lines show observed spectra and dashed lines show fits to a linear combination of the zeroth and first derivatives of the absorption band.

To analyze the χ-dependence of the NIR EA spectra, we first performed a least-squares fitting of the FTIR spectrum [Fig. 3(a)] using a Gaussian band shape plus a linear baseline. Another Gaussian function was included in the fit to account for a small satellite feature that the $\nu_1 + \nu_4$ combination band accompanies at its higher-frequency side ($\sim$4260 cm^{-1}). However, because the absorbance change of the satellite band is most likely below our detection limit, we did not include this component in the subsequent fitting of the EA spectra. The χ-dependent EA spectra [Fig. 3(b)] were then fitted to a linear combination of the zeroth and first derivatives of the absorption band with the peak position and bandwidth fixed to the values obtained from the above fitting procedure. It turned out that the contribution of the second-derivative component was negligible; therefore, we included only the zeroth and first derivatives in the fitting. The coefficient for the zeroth-derivative component, which arises from both the orientational polarization [Eq. (8)] and the electronic polarization [Eq. (11)], is plotted as a function of χ in Fig. 4. The plot was fitted assuming a function $a(1 - 3\cos^2\chi) + b$, which gives $a = (5.3 \pm 1.9) \times 10^{-6}$ and $b = (1.0 \pm 1.0) \times 10^{-6}$. The value of b is fairly small compared with that of a. Referring to Eq. (11), this result suggests that the coefficient a can be attributed almost entirely to the orientational polarization a_{OP} ($\gg a_{\text{EP}}$). The value of a_{OP} for the combination band is therefore obtained to be $(5.3 \pm 1.9) \times 10^{-6}$.

The contribution of the first-derivative component is significant at all χ studied, resulting in the redshift of the peak.

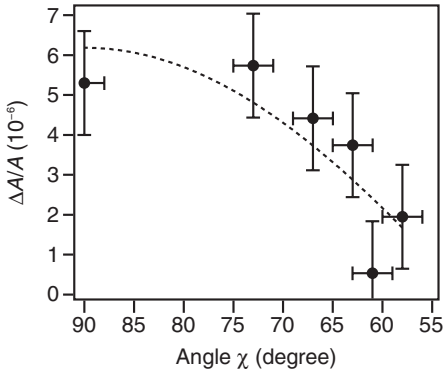

FIG. 4. Angle χ dependence of the coefficient for the zeroth derivative determined by the spectral fitting for the $\nu_1 + \nu_4$ combination band of chloroform. The dashed line is the fit to $a(1 - 3\cos^2\chi) + b$. To facilitate comparison with Fig. 3, χ is plotted such that it increases toward the left.

The first-derivative coefficient B_χ has many terms involving $\Delta\boldsymbol{\mu}$, $\Delta\boldsymbol{\alpha}$, and $\mathbf{A}$.[36] Unfortunately, the poor spectral resolution in our measurement (16 cm^{-1}) and low S/N prevent us from analyzing B_χ quantitatively. By further improving the apparatus, we will be able to examine the coefficient B_χ and address how the electronic characteristics of the vibrational states involved in combination transitions are affected by electric fields.[39,44]

C. EA spectra in the fundamental band region

We now have derived $(\Delta A/A)_{OP}$ experimentally, so it is in principle possible to evaluate angle η using Eq. (8). In so doing, however, the dipolar interaction parameter γ needs to be determined. As is evident from Eq. (9), determination of γ requires the strength of the local field, F. The local field $\mathbf{F}$ differs from the externally applied electric field $\mathbf{F}_{ext}$ ($|\mathbf{F}_{ext}| \approx 0.13$ MV cm^{-1} in the present case) and the difference is corrected for by introducing the local field correction factor f: $\mathbf{F} = f\mathbf{F}_{ext}$. In most cases, f cannot be obtained experimentally with high accuracy. In fact, molecular parameters such as $\Delta\mu$ and $\Delta\alpha$ have often been reported in terms of factors of f.[36,45–47] In our previous work, we circumvented this problem by using an intensity standard.[18,33] Here too, we adopt a similar approach: namely, the absorbance changes of the CH-stretching and CH-bending modes with known values of η (0° and 90°, respectively) are analyzed and used to determine the value of γ without going through the direct evaluation of f.

1. CH-stretching mode ν_1

Figure 5 shows a rather unexpected, interesting χ-dependence of the absorbance change for the ν_1 mode. As described above, the absorption band of the ν_1 mode [Fig. 5(a)] was fitted to a Gaussian function, followed by a fitting of the χ-dependent EA IR spectra [Fig. 5(b)] with a linear combination of the zeroth, first, and second derivatives of the absorption band. The resulting zeroth-derivative coefficient is plotted as a function of χ in Fig. 6. A very small, positive $\Delta A/A$ of $\sim 2.5 \times 10^{-6}$ is observed at $\chi = 90°$, and $\Delta A/A$ drastically increases as χ decreases. Equation (8) with $\eta = 0°$ predicts

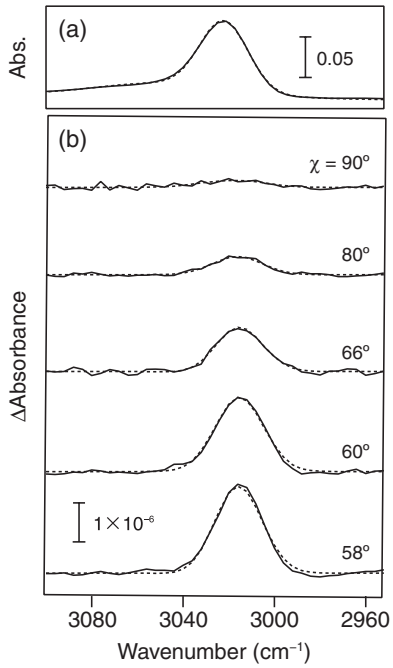

FIG. 5. IR spectrum (a) and EA spectra (b) of liquid chloroform in the CH-stretching (ν_1) band region. The EA spectra were measured at $\chi = 58°$, 60°, 66°, 80°, and 90° (normal incidence). Solid lines show observed spectra and dashed lines show fits to a linear combination of the zeroth, first, and second derivatives of the absorption band.

a negative $\Delta A/A$ value for the orientational polarization at $\chi = 90°$. Our observation is in apparent contrast with this prediction, suggesting a significant contribution of the electronic polarization to the zeroth-derivative term. Unlike the case of the combination band, the observed absorbance change cannot be attributed solely to the orientational polarization. We fitted the χ-dependence plot (Fig. 6) to $a(1 - 3\cos^2\chi) + b$, yielding $a = (-2.7 \pm 0.6) \times 10^{-5}$ and $b = (2.9 \pm 0.6) \times 10^{-5}$. This value of a includes both orientational polarization (a_{OP}) and electronic polarization (a_{EP}) contributions ($a = a_{OP} + a_{EP}$), whereas the coefficient b originates solely from electronic polarization ($b = b_{EP}$).

To extract the contribution of the orientational polarization, we approximate Eq. (11) by assuming that only one

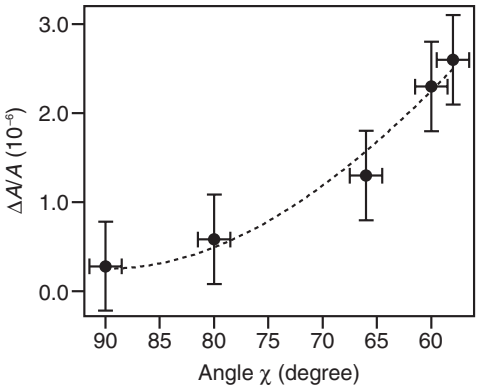

FIG. 6. Angle χ dependence of the coefficient for the zeroth derivative determined by the spectral fitting for the ν_1 band of chloroform. The dashed line is the fit to $a(1 - 3\cos^2\chi) + b$. To facilitate comparison with Fig. 5, χ is plotted such that it increases toward the left.

particular component of the transition polarizability **A** is dominant and the other elements are negligible. This one-dimensional approximation was previously applied to the C≡N stretch of nitriles and was found to be not always valid.[45] However, the one-dimensional approximation should hold for the CH single bond of chloroform, which involves only σ-electrons unlike the C≡N bond of nitriles. Letting the CH bond be along with the molecule-fixed z-axis (see the coordinate system given in Fig. 1), we can simplify Eq. (11) as

$$\left(\frac{\Delta A}{A}\right)_{\mathrm{OP}} = \frac{F^2}{30\,|\mathbf{m}|^2}\left[10A_{zz}^2 - 4A_{zz}^2(1 - 3\cos^2\chi)\right], \quad (12)$$

where A_{zz} represents the zz-element of the transition polarizability tensor **A**. The first term, $10A_{zz}^2$, in the square brackets corresponds to the coefficient b ($= b_{\mathrm{EP}}$), whereas the prefactor of the $1 - 3\cos^2\chi$ term, $(-4A_{zz}^2)$, corresponds to the coefficient a_{EP}. Under the approximation of Eq. (12), the ratio $a_{\mathrm{EP}}/b_{\mathrm{EP}}$ is theoretically equal to -0.4. Using this relation, we calculate the value of the a_{EP} to be $(2.9 \times 10^{-5}) \times (-0.4) = -1.16 \times 10^{-5}$. Subtraction of this value from the fitted result of a ($= a_{\mathrm{OP}} + a_{\mathrm{EP}}$) leaves a_{OP} of $(-1.5 \pm 0.6) \times 10^{-5}$ for the CH-stretching band. After the contribution of the electronic polarization has been removed appropriately, the $\Delta A/A$ value for the orientational polarization becomes negative as predicted by Eq. (8) with $\eta = 0°$.

The significant contribution of the electronic polarization to the CH-stretching ΔA signal is a consequence of a large field dependence of the transition moment, i.e., large transition polarizability. This, in turn, means that the CH-stretching vibration is highly susceptible to the surrounding electrostatic environment. Despite being the most fundamental chemical bond, the CH bond has not been discussed in this context. We need more experiments to clarify whether this characteristic is unique to chloroform or not.

2. CH-bending mode ν_4

Similarly, we measured the field-induced absorbance change for the ν_4 mode (Fig. 7). The observed IR EA spectrum looks quite different from those for the ν_1 band and the $\nu_1 + \nu_4$ combination band. As χ decreases from normal incidence, the depletion of the area intensity of the ν_4 band is observed, indicative of the absorbance change originating from the orientational polarization. At $\chi < 66°$, the ΔA spectrum is dominated by a first-derivative shape, indicating that electric field application induces a redshift of the CH-bending mode. We performed least-squares fitting of the ΔA spectra with a linear combination of the zeroth, first, and second derivatives of the absorption band and subsequently attempted to fit the χ-dependence of the resulting zeroth-derivative coefficient with $a(1 - 3\cos^2\chi) + b$. The fitting yielded $b < 0$, but it is inconsistent with the prediction by Eq. (11) that the χ-independent component of the electronic polarization ΔA signal must be non-negative. We attribute this observation to a large variation of the refractive index caused by the strong absorption of the CH-bending mode. Refractive index-corrected angle χ may largely depend on the wavenumber and distort the spectrum. Fortunately, the $\chi = 90°$ spectrum can be free from this undesirable possibility, so we regard the $\Delta A/A$ of $(4.3 \pm 1.0) \times 10^{-6}$ at $\chi = 90°$, determined by the fitting, as arising from the orientational polarization response of the CH-bending mode. Note that as far as area intensity is concerned, the first-derivative term (due to electronic polarization) does not affect the above treatment.

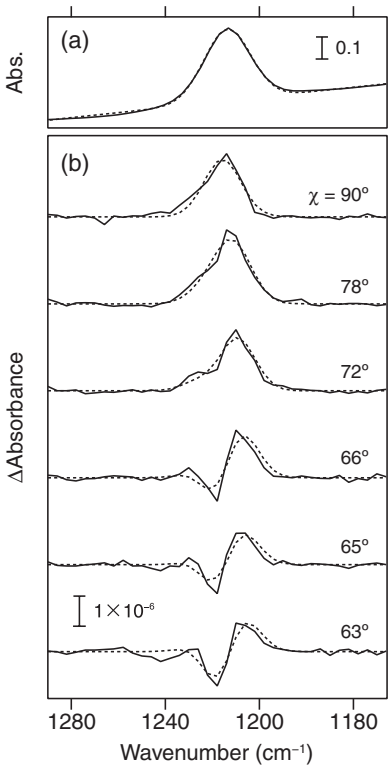

FIG. 7. IR spectrum (a) and EA spectra (b) of liquid chloroform in the CH-bending (ν_4) band region. The EA spectra were measured at $\chi = 63°$, 65°, 66°, 72°, 78°, and 90° (normal incidence). Solid lines show observed spectra and dashed lines show fits to a linear combination of the zeroth, first, and second derivatives of the absorption band.

D. Determination of η for the combination band

The experimentally determined values of a_{OP} for the three IR bands are summarized: $a_{\mathrm{OP}} = (-1.5 \pm 0.6) \times 10^{-5}$ for ν_1; $(4.3 \pm 1.0) \times 10^{-6}$ for ν_4; and $(5.3 \pm 1.9) \times 10^{-6}$ for $\nu_1 + \nu_4$. Using Eq. (8), the value of γ^2 for each of the ν_1 and ν_4 modes is obtained to be $(9.0 \pm 3.0) \times 10^{-5}$ and $(5.2 \pm 1.2) \times 10^{-5}$, respectively. Ideally, the two fundamental modes should give an identical γ^2 value within experimental uncertainties. The discrepancy between the two experimental values is probably due to the subtraction procedure we employed to estimate a_{OP} for the CH-stretching mode, which could increase relative errors. Here, we use for further calculations the average of the two γ^2 values as an *ad hoc* solution for the discrepancy, i.e., $\bar{\gamma}^2 = (7.1 \pm 2.1) \times 10^{-5}$. Using Eq. (8) again with $(\Delta A/A)_{\mathrm{OP}} = a_{\mathrm{OP}} = (5.3 \pm 1.9) \times 10^{-6}$ and $\bar{\gamma}^2 = (7.1 \pm 2.1) \times 10^{-5}$, we finally have $\eta = (79 \pm 14)°$ for the $\nu_1 + \nu_4$ combination band of chloroform. We have successfully demonstrated the ability of NIR EA spectroscopy to experimentally determine the direction of the transition moment for a combination band of a liquid. The $\eta = 79°$ so obtained indicates that the transition moment for the

TABLE I. Calculated vibrational frequencies, first derivatives of the dipole moment, and mechanical anharmonicity terms of the ν_1 and ν_4 fundamentals.

Mode	Frequency[a] (cm^{-1})	$\lvert(\partial\mu/\partial Q)_0\rvert$ (D $Å^{-1}$)	$\lvert\mathbf{m}^{MA}\rvert$ (D)
CH stretch, ν_1	3189	0.099	8.0×10^{-6}
CH bend, ν_4	1247	0.79	5.8×10^{-3}

[a]Unscaled.

combination band is nearly perpendicular to the CH bond axis of chloroform. Therefore, we can conclude that the mechanical anharmonicity of the CH-bending mode ($\mathbf{m}^{MA}_{bend}$), which is perpendicular to the CH bond, plays a major role in the vibrational coupling between the two modes. The observed anharmonic shift of 19 cm^{-1} for the $\nu_1 + \nu_4$ combination band implies that the contribution of the mechanical anharmonicity does exist because the electrical anharmonicity does not cause any frequency shift.

The minor contribution of the CH-stretching mode to the mechanical anharmonicity can be readily rationalized by considering the symmetry of the potential energy surface $V(Q_{stretch}, Q_{bend})$. As is evident from Fig. 1(b), $V(Q_{stretch}, Q_{bend})$ should be symmetric with respect to the normal coordinate Q_{bend}, i.e., $V(Q_{stretch}, Q_{bend}) = V(Q_{stretch}, -Q_{bend})$. Due to this symmetry property, the Taylor expansion of $V(Q_{stretch}, Q_{bend})$ should not contain the term $Q^2_{stretch}Q_{bend}$, resulting in negligible $(\partial^3 V/\partial Q^2_{stretch}\partial Q_{bend})_0$ and hence very small $\mathbf{m}^{MA}_{stretch}$ [recall Eq. (5)]. DFT calculation results discussed in Subsection IV E are consistent with this account.

E. Mechanical vs electrical anharmonicity: Insight from DFT calculation

We now ask which of the CH-bending mechanical anharmonicity $\mathbf{m}^{MA}_{bend}$ and the electrical anharmonicity $\mathbf{m}^{EA}$ predominates. To address this question, the potential energy surface $V(q_{stretch}, q_{bend})$ and the dipole moment function $\mu(q_{stretch}, q_{bend})$ of a bare, gas-phase chloroform molecule were computed using the DFT/B3LYP method. Calculated vibrational frequencies and first derivatives of the dipole moment for the ν_1 and ν_4 modes are summarized in Table I. Figure 8 shows a contour plot of the calculated potential energy surface $V(q_{stretch}, q_{bend})$. It was fitted well with a two-dimensional third-order polynomial, yielding $\partial^3 V/\partial q_{stretch}\partial q^2_{bend} = 0.93$ hartree $Å^{-3}$ and $\partial^3 V/\partial q^2_{stretch}\partial q_{bend} = 0.01$ hartree $Å^{-3}$. These values are in reasonable agreement with those reported by Cho and co-workers.[27] The quartic and higher-order dependence on the normal coordinates $q_{stretch}$ and q_{bend} can possibly contribute to the potential energy as Reimers and Hush[48] showed in their benchmark calculations. However, because the evaluation of those terms using the present DFT-based method may have large uncertainty, they were not incorporated in the above fitting. Substituting the calculated results into Eqs. (5) and (6), we obtain $\left|\mathbf{m}^{MA}_{stretch}\right| = 8.0 \times 10^{-6}$ D and $\left|\mathbf{m}^{MA}_{bend}\right| = 5.8 \times 10^{-3}$ D. Consistent with the experiment, the DFT calculation also shows that $\mathbf{m}^{MA}_{stretch}$ is negligible relative to $\mathbf{m}^{MA}_{bend}$.

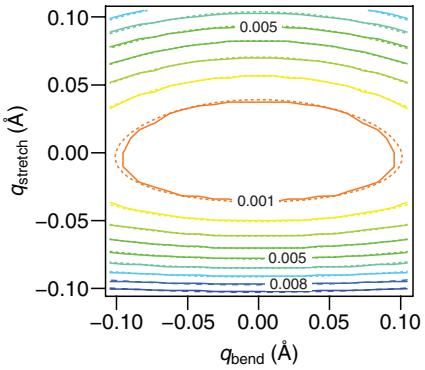

FIG. 8. Contour plot of the potential energy surface $V(q_{stretch}, q_{bend})$ in units of hartree computed for an isolated chloroform molecule. Solid lines are calculated results and dashed lines are the fit to a two-dimensional third-order polynomial.

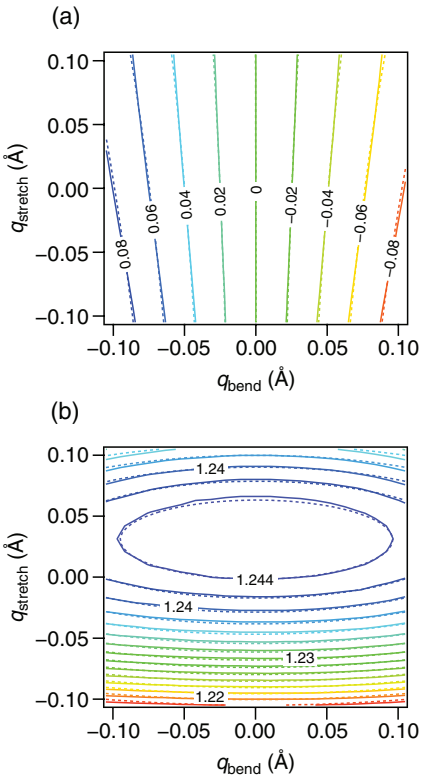

FIG. 9. Contour plots of the dipole moment function $\mu(q_{stretch}, q_{bend})$ in units of Debye computed for an isolated chloroform molecule: (a) the y-component μ_y and (b) the z-component μ_z. Solid lines are calculated results and dashed lines are the fit to a two-dimensional second-order polynomial.

Figure 9 displays contour plots of the y- and z-components of the calculated dipole moment, μ_y [Fig. 9(a)] and μ_z [Fig. 9(b)]. Here, the z-axis is taken to coincide with the CH bond [see Fig. 1(a)]. A fitting analysis with two-dimensional second-order polynomials (neglecting the third and higher-order terms) yields $(\partial\mu_y/\partial q_{stretch}\partial q_{bend})_0 = 1.2$ D $Å^{-2}$ and $(\partial\mu_z/\partial q_{stretch}\partial q_{bend})_0 \cong 0$ D $Å^{-2}$. This result can be qualitatively accounted for by the following argument: The z-component of the dipole moment function, $\mu_z(q_{stretch}, q_{bend})$, is symmetric with respect to q_{bend} and has to include q_{bend} only at even orders. Therefore, $(\partial^2\mu_z/\partial q_{stretch}\partial q_{bend})_0 \approx 0$. In contrast, the y-component μ_y can have an odd dependence on Q_{bend} and therefore $(\partial^2\mu_y/\partial q_{stretch}\partial q_{bend})_0$ can be nonzero. By symmetry, we expect $(\partial^2\mu_x/\partial q_{stretch}\partial q_{bend})_0 \neq 0$ as well.

The above symmetry consideration leads us to the conclusion that $\mathbf{m}^{\mathrm{EA}}$ is perpendicular to the CH bond axis, as is $\mathbf{m}^{\mathrm{MA}}_{\mathrm{bend}}$. In other words, $\mathbf{m}^{\mathrm{MA}}_{\mathrm{bend}}$ and $\mathbf{m}^{\mathrm{EA}}$ are indistinguishable on the basis of solely the direction of the combination transition moment.

Upon substitution of $(\partial\mu_x/\partial q_{\mathrm{stretch}}\partial q_{\mathrm{bend}})_0 \cong (\partial\mu_y/\partial q_{\mathrm{stretch}}\partial q_{\mathrm{bend}})_0 = 1.2$ D Å^{-2} and $(\partial\mu_z/\partial q_{\mathrm{stretch}}\partial q_{\mathrm{bend}})_0 \cong 0$ D Å^{-2} into Eq. (7), the magnitude of $\mathbf{m}^{\mathrm{EA}}$ becomes 1.0×10^{-2} D, which is comparable to $\mathbf{m}^{\mathrm{MA}}_{\mathrm{bend}} = 5.8 \times 10^{-3}$ D. It is generally accepted that for high-frequency intramolecular vibrations, anharmonic coupling is usually dominated by the mechanical anharmonicity.[9,49] In addition, the electrical anharmonicity seems to play a crucial role only in hydrogen-bonded systems[30,50,51] and other types of molecular complexes,[52] in which non-covalent interactions are involved. However, the present DFT calculations suggest that both $\mathbf{m}^{\mathrm{MA}}_{\mathrm{bend}}$ and $\mathbf{m}^{\mathrm{EA}}$ may contribute equally to the anharmonic coupling between the ν_1 and ν_4 modes. In fact, Kwak and co-workers[53] analyzed cross-peaks of the C–C and C≡N stretching modes of acetonitrile obtained with doubly vibrationally enhanced IR–IR–visible four-wave-mixing spectroscopy and reached a similar conclusion that mechanical and electrical anharmonicities are both important to account for the anharmonic coupling of those modes.

V. CONCLUDING REMARKS

Our proof-of-principle study of NIR EA spectroscopy presented in this paper has several important implications. First, the direction of the transition moment of a combination band that can be determined by our method should serve as a critical test of theoretical calculations in which the breakdown of the double harmonic approximation (i.e., harmonic potential plus linear dependence of the dipole moment) is explicitly considered. Another implication is that NIR EA spectroscopy could be powerful for studying the electric field effects on vibrational modes such as the OH-stretching mode of water, whose fundamentals occurring in the MIR region are too strong to be accurately measured with absorption spectroscopy. Further improvement in the sensitivity of the apparatus will enable us to apply NIR EA spectroscopy to molecular systems other than liquid chloroform. Last, NIR EA spectroscopy may also be used to assign as yet unidentified NIR bands. Polyatomic molecules have many fundamentals and anharmonic coupling among them produces a far larger number of overtones and combination bands. This complexity as well as their weak signal intensity has been a hurdle that prevents spectroscopists from fully utilizing rich information buried under the NIR region. We believe that NIR EA spectroscopy would assist in overcoming this hurdle by looking into the direction of the transition moment.

ACKNOWLEDGMENTS

The authors are grateful to the National Chiao Tung University for funding the ''Ultimate Spectroscopy and Imaging'' project. They also thank Mitsubishi Plastics for providing them with the polymer film used as a spacer. S.S. wishes to thank partial support from the National Science Council of Taiwan (Grant No. NSC98-2113-M-009-011-MY2).

[1] D. D. Dlott, Chem. Phys. **266**, 149 (2001).
[2] R. M. Stratt and M. Maroncelli, J. Phys. Chem. **100**, 12981 (1996).
[3] A. Morresi, L. Mariani, M. R. Distefano, and M. G. Giorgini, J. Raman Spectrosc. **26**, 179 (1995).
[4] D. W. Oxtoby, Annu. Rev. Phys. Chem. **32**, 77 (1981).
[5] A. Barth and C. Zscherp, Quart. Rev. Biophys. **35**, 369 (2002).
[6] Y. S. Kim and R. M. Hochstrasser, J. Phys. Chem. B **113**, 8231 (2009).
[7] R. R. Ernst, G. Bodenhausen, and A. Wokaun, *Principles of Nuclear Magnetic Resonances in One and Two Dimensions* (Clarendon, Oxford, 1987).
[8] M. Khalil and A. Tokmakoff, Chem. Phys. **266**, 213 (2001).
[9] O. Golonzka, M. Khalil, N. Demirdöven, and A. Tokmakoff, Phys. Rev. Lett. **86**, 2154 (2001).
[10] M. Khalil, N. Demirdöven, and A. Tokmakoff, J. Phys. Chem. A **107**, 5258 (2003).
[11] R. M. Hochstrasser, Proc. Natl. Acad. Sci. U.S.A. **104**, 14190 (2007).
[12] M. Cho, Chem. Rev. **108**, 1331 (2008).
[13] *Near-Infrared Spectroscopy: Principles, Instruments, Applications*, edited by H. W. Siesler, Y. Ozaki, S. Kawata, and H. M. Heise (Wiley-VCH, Weinheim, 2002).
[14] K. Iwata and H. Hamaguchi, Appl. Spectrosc. **44**, 1431 (1990).
[15] T. Yuzawa, C. Kato, M. W. George, and H. Hamaguchi, Appl. Spectrosc. **48**, 684 (1994).
[16] S. Yabumoto, S. Shigeto, Y.-P. Lee, and H. Hamaguchi, Angew. Chem., Int. Ed. **49**, 9201 (2010).
[17] H. Hiramatsu and H. Hamaguchi, Appl. Spectrosc. **58**, 355 (2004).
[18] W.-C. Wang and S. Shigeto, J. Phys. Chem. A **115**, 4448 (2011).
[19] T. Shimanouchi, *Tables of Molecular Vibrational Frequencies. Consolidated Volume I* (U.S. Department of Commerce, NSRDS-NBS 39, Washington, D.C., 1972).
[20] H. J. Bakker, P. C. M. Planken, L. Kuipers, and A. Lagendijk, J. Chem. Phys. **94**, 1730 (1991).
[21] H. Graener, R. Zürl, and M. Hofmann, J. Phys. Chem. B **101**, 1745 (1997).
[22] E. L. Sibert III and R. Rey, J. Chem. Phys. **116**, 237 (2002).
[23] A. Tokmakoff, M. J. Lang, D. S. Larsen, G. R. Fleming, V. Chernyak, and S. Mukamel, Phys. Rev. Lett. **79**, 2702 (1997).
[24] K. Tominaga and K. Yoshihara, Phys. Rev. A **55**, 831 (1997).
[25] K. Tominaga and K. Yoshihara, J. Phys. Chem. A **102**, 4222 (1998).
[26] K. Okumura and Y. Tanimura, Chem. Phys. Lett. **278**, 175 (1997).
[27] S. Hahn, K. Park, and M. Cho, J. Chem. Phys. **111**, 4121 (1999).
[28] K. Park, M. Cho, S. Hahn, and D. Kim, J. Chem. Phys. **111**, 4131 (1999).
[29] P. Kukura, R. Frontiera, and R. A. Mathies, Phys. Rev. Lett. **96**, 238303 (2006).
[30] K. Ishii, S. Takeuchi, and T. Tahara, J. Chem. Phys. **131**, 044512 (2009).
[31] G. Herzberg, *Molecular Spectra and Molecular Structure: II. Infrared and Raman Spectra of Polyatomic Molecules* (Van Nostrand, New York, 1945).
[32] W. Liptay, Angew. Chem., Int. Ed. **8**, 177 (1969).
[33] S. Shigeto, H. Hiramatsu, and H. Hamaguchi, J. Phys. Chem. A **110**, 3738 (2006).
[34] F. Dong and R. E. Miller, Science **298**, 1227 (2002).
[35] G. U. Bublitz and S. G. Boxer, Annu. Rev. Phys. Chem. **48**, 213 (1997).
[36] S. A. Locknar and L. A. Peteanu, J. Phys. Chem. B **102**, 4240 (1998).
[37] E. Jalviste and N. Ohta, J. Photochem. Photobiol. C **8**, 30 (2007).
[38] M. Ponder and R. Mathies, J. Phys. Chem. **87**, 5090 (1983).
[39] S. A. Andrews and S. G. Boxer, J. Phys. Chem. A **106**, 469 (2002).
[40] J. R. Reimers, J. Zeng, and N. S. Hush, J. Phys. Chem. **100**, 1498 (1996).
[41] A. D. Becke, J. Chem. Phys. **98**, 5648 (1993).
[42] C. Lee, W. Yang, and R. G. Parr, Phys. Rev. B **37**, 785 (1988).
[43] M. J. Frisch, G. W. Trucks, H. B. Schlegel *et al.*, GAUSSIAN 09, Revision A.02, Gaussian, Inc., Wallingford, CT, 2009.
[44] S. H. Brewer and S. Franzen, J. Chem. Phys. **119**, 851 (2003).
[45] S. S. Andrews and S. G. Boxer, J. Phys. Chem. A **104**, 11853 (2000).
[46] T. Nakabayashi and N. Ohta, Chem. Lett. **34**, 1194 (2005).
[47] E. S. Park and S. G. Boxer, J. Phys. Chem. B **106**, 5800 (2002).
[48] J. R. Reimers and N. S. Hush, J. Phys. Chem. A **103**, 10580 (1999).
[49] P. Geerlings, D. Berckmans, and H. P. Figeys, J. Mol. Struct. **57**, 283 (1979).
[50] E. Marechal and S. Bratos, J. Chem. Phys. **68**, 1825 (1978).
[51] S. M. Melikova, A. J. Inzebejkin, D. N. Shchepkin, and A. koll, J. Mol. Struct. **552**, 273 (2000).
[52] R. Guo, F. Fournier, P. M. Donaldson, E. M. Gardner, I. R. Gould, and D. R. Klug, Phys. Chem. Chem. Phys. **11**, 8417 (2009).
[53] K. Kwak, S. Cha, M. Cho, and J. C. Wright, J. Chem. Phys. **117**, 5675 (2002).